Supplementary Information

Bayesian optimization with constraint on passed charge for multiparameter screening of electrochemical reductive carboxylation in a flow microreactor

Yuki Naito,[a†] Masaru Kondo,[b,c†] Yuto Nakamura,[a] Naoki Shida,[a] Kazunori Ishikawa,[d] Takashi Washio,[c,e] Shinobu Takizawa,[c,e*] Mahito Atobe[a*]*

[a] Graduate School of Science and Engineering, Yokohama National University, 79-1 Tokiwadai, Hodogaya-ku, Yokohama, 240-8501, Japan.

[b] Department of Materials Science and Engineering, Graduate School of Science and Engineering, Ibaraki University, Hitachi 316-8511, Ibaraki, Japan.

[c] Department of Synthetic Organic Chemistry, Osaka University, Mihogaoka, Ibaraki, Osaka 567-0047, Japan

[d] Department of Reasoning for Intelligence, SANKEN, Osaka University, Japan.

[e] Artificial Intelligence Research Center, SANKEN, Osaka University, Japan.

† The authors contributed equally

E-mail: washio@ar.sanken.osaka-u.ac.jp (Prof. T. Washio), taki@sanken.osaka-u.ac.jp (Prof. S. Takizawa), atobe@ynu.ac.jp (Prof. M. Atobe)

Contents

1. General considerations

All chemicals were used without further purification. Compounds **1a–c** and **2a** were purchased from commercial sources. Compounds **1d–f** and **2b–f** were synthesized according to reported procedures. A silicone oil bath was used as a heat source for the reactions. Flow electrolysis was conducted with a homemade electrochemical microreactor. During the electrosynthesis, a substrate solution was introduced to the microreactor by a syringe pump (KD Scientific KDS100, Muromachi Kikai). The electrochemical carboxylations were conducted using a potentiogalvanostat (HABF-501A, Hokuto Denko). High-performance liquid chromatography (HPLC) analysis for **2a** was performed with an Inertsil ODS-4 column (GL Sciences) using a mixture of H_2O/MeCN/H_3PO_4 (90/10/0.1%) as the mobile phase. HPLC analyses for **2b–f** were performed with an Inertsil ODS-4 column (GL Sciences) using a mixture of H_2O/MeCN/H_3PO_4 (60/40/0.1%) as the mobile phase. All liquid chromatograms were recorded using a liquid chromatography (LC) workstation (LabSolutions DB, Shimadzu). Gas chromatography analyses were performed using a Shimadzu gas chromatograph (GC2014) equipped with a SHINCARBON-ST 50-80 G-1165 column (Shimadzu). He was used as a carrier gas for the GC analyses. ^{1}H NMR spectra were recorded on a Bruker DRX-500 (500 MHz) spectrometer using tetramethylsilane (TMS) as an internal standard with the solvent resonance ($CDCl_3$: δ 7.26, DMSO: δ 2.50). The chemical shifts for ^{1}H NMR spectra are given in δ (ppm) relative to the internal TMS. Multiplicities are abbreviated as singlet (s), doublet (d), triplet (t), doublet of triplets (dt), and multiplet (m). Chronoamperometry was performed using a CH Instruments ALS/H electrochemical analyzer (model 630c).

2. Synthesis

2-1. General procedure for the synthesis of imines (1d–f) as authentic samples for HPLC analysis

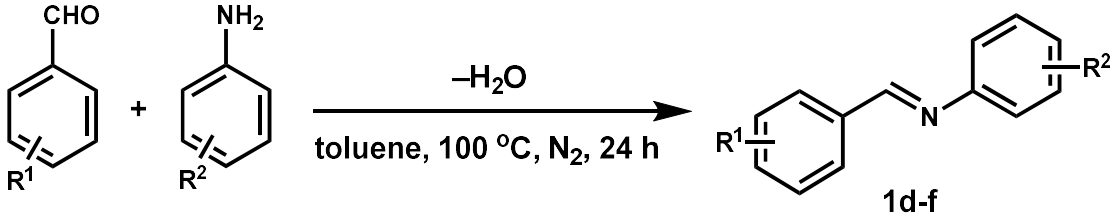

Imines **1d–f** were synthesized according to a reported procedure.[1] Anilines (5.0 mmol, 1.0 equiv.) were added to a solution of aldehyde (5.0 mmol, 1.0 equiv.) in dry toluene (5.0 mL) and molecular sieves (MS4A, 1.0 g). The reaction mixture was heated to reflux and reacted for 24 h under a N_2 atmosphere, then cooled to room temperature and filtered through Celite. The solvent was removed under reduced pressure. The residue was purified by column chromatography using silica gel (hexane/Et_2O 50:1) to afford products **1d–f**.

N-Benzylidene-4-methoxyaniline (**1d**):[2] yellow solid, 0.99 g, 79% yield. ^{1}H NMR (500 MHz; $CDCl_3$): δ 8.49 (s, 1H), 7.89 (dt, J = 4.0, 3.0 Hz, 2H), 7.48–7.45 (m, 3H), 7.23–7.26 (m, 2H), 6.96–6.92 (m, 2H), 3.84 (s, 3H).

N-(4-(Trifluoromethyl)benzylidene)aniline (**1e**):[3] yellow solid, 0.85 g, 81% yield. ^{1}H NMR (500 MHz; $CDCl_3$): δ 8.52 (s, 1H), 8.03 (d, J = 7.9 Hz, 2H), 7.74 (d, J = 7.9 Hz, 2H), 7.44–7.40 (m, 2H), 7.29–7.20 (m, 1H).

N-Benzylidene-4-trifluoromethylaniline (**1f**):[2] yellow solid, 0.73 g, 59% yield. ^{1}H NMR (500 MHz; $CDCl_3$): δ 8.43 (s, 1H), 7.93–7.90 (m, 2H), 7.65 (dd, J = 8.8, 0.6 Hz, 2H), 7.53–7.48 (m, 3H), 7.25 (s, 2H).

2-2. General procedure for the synthesis of α-amino acids (2b, 2c, 2e, and 2f) as authentic samples for HPLC analysis

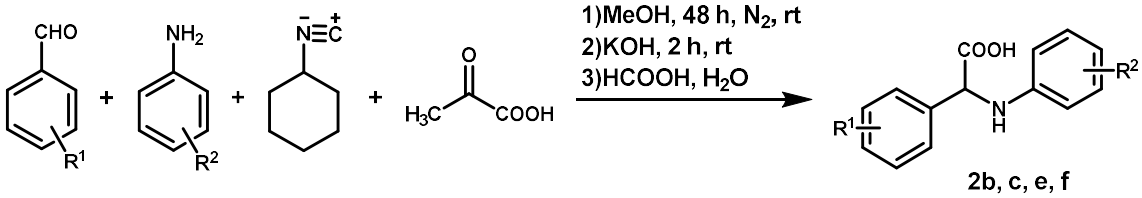

α-Amino acids **2b**, **2c**, **2e**, and **2f** were synthesized according to a method reported in the literature.[4] A solution of aldehyde (5.0 mmol, 1.0 equiv.) and aniline (5.0 mmol, 1.0 equiv.) in MeOH (20 mL) was stirred for 10 min at room temperature. After the reaction, a mixture of pyruvic acid (5.0 mmol, 1.0 equiv.) and cyclohexyl isocyanide (5.0 mmol, 1.0 equiv.) was added and the resultant mixture was stirred at room temperature for 48 h under a N_2 atmosphere. The reaction mixture was then treated with a solution of KOH (6.0 mmol, 1.2 equiv.) in MeOH (4.0 mL). After the mixture was stirred for 2 h at room temperature, the solvent was removed under reduced pressure and the residue was dissolved in water (30 mL) and washed with $CHCl_3$ (30 mL). The aqueous phase was acidified to pH 4 by addition of formic acid. The resultant suspension was filtered, and the collected solid product was washed with water and dried to give α-amino acids **2b**, **2c**, **2e**, and **2f**.

α-(Phenylamino)benzeneacetic acid (**2b**):[4] yellow solid, 0.30 g, 26% yield. ^{1}H NMR (500 MHz, DMSO-d_6): δ 7.50 (m, 2H), 7.35 (t, J = 7.4 Hz, 2H), 7.31–7.26 (m, 1H), 7.04–7.01 (dd, J = 8.5, 7.3 Hz, 2H), 6.64 (d, J = 8.5 Hz, 2H), 6.53 (t, J = 7.3 Hz, 1 H), 5.06 (s, 1 H).

4-Methoxy-α-(phenylamino)benzeneacetic acid (**2c**):[4] yellow solid, 0.18 g, 14% yield. ^{1}H NMR (500 MHz; DMSO-d_6): δ 6.91 (d, J = 8.4 Hz, 2H), 6.63 (d, J = 8.4 Hz, 2H), 6.53 (t, J = 7.1 Hz, 2H), 4.99 (s, 1H), 3.76–3.70 (m, 3H).

α-(Phenylamino)-4-(trifluoromethyl)benzeneacetic acid (**2e**):[5] yellow solid, 0.33 g, 22% yield. ^{1}H NMR (500 MHz; DMSO-d_6): δ 7.77–7.72 (m, 4H), 7.72–7.63 (m, 1H), 7.04 (t, J = 8.0 Hz, 2H), 6.66 (d, J = 8.0 Hz, 2H), 6.56 (t, J = 7.3 Hz, 1H), 5.26 (s, 1H).

α-[(4-Trifluoromethylphenyl)amino]benzeneacetic acid (**2f**):[5] yellow solid, 0.65 g, 44% yield. ^{1}H NMR (500 MHz; DMSO-d_6): δ 7.51 (d, J = 8.0 Hz, 2H), 7.41–7.30 (m, 6H), 6.98 (d, J = 6.8 Hz, 1H), 6.79 (d, J = 8.0 Hz, 2H), 5.20 (d, J = 6.8 Hz, 1H).

2-3. Procedure for the synthesis of α-amino acid 2d as authentic samples for HPLC analysis

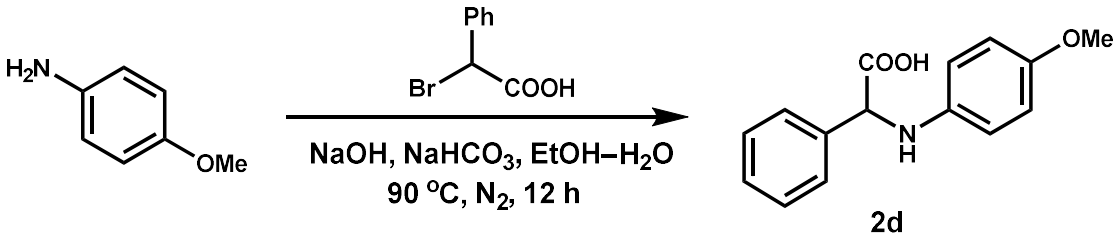

α-Amino acid **2d** was synthesized according to a method reported in the literature.[6,7] α-Bromophenylacetic acid (1.1 g, 5.0 mmol), $NaHCO_3$ (0.42 g, 5.0 mmol), and *p*-anisidine (0.74 g, 6.0 mmol) in ethanol (5.0 mL) were added to a solution of NaOH (0.20 g, 5.0 mmol) in water (20 mL) at 0 °C. After the mixture was reacted at 90 °C for 12 h under a N_2 atmosphere, the solution was concentrated and acidified with 1 M hydrochloric acid to pH = 4 at 0 °C. The precipitate was collected by filtration, dried in vacuo, and triturated with 10% Et_2O in hexane to afford α-amino acid **2d**.

α-[(4-Methoxyphenyl)amino]benzeneacetic acid (**2d**):[8] yellow solid, 0.15 g, 12% yield. ^{1}H NMR (500 MHz; DMSO-d_6): δ 7.48 (d, J = 7.6 Hz, 2H), 7.35–7.29 (m, 1H), 7.28–7.23 (m, 1H), 6.67–6.63 (m, 2H), 6.59–6.55 (m, 2H), 4.89 (s, 1H).

3. Fabrication of electrochemical flow microreactor

The electrochemical flow microreactor was constructed with a Pt plate (3 cm × 3 cm) and a glassy carbon (GC) plate (3 cm × 3 cm) (Fig. S1). Multiple sheets of 10 or 80 μm-thick double-faced adhesive type were overlapped to make a spacer of the desired thickness. A spacer was used to leave a rectangular channel exposed (1 cm × 3 cm), and the two electrodes were simply sandwiched together. After Teflon tubing was connected to the inlets and outlet, the reactor was sealed with epoxy resin (Fig. S2).

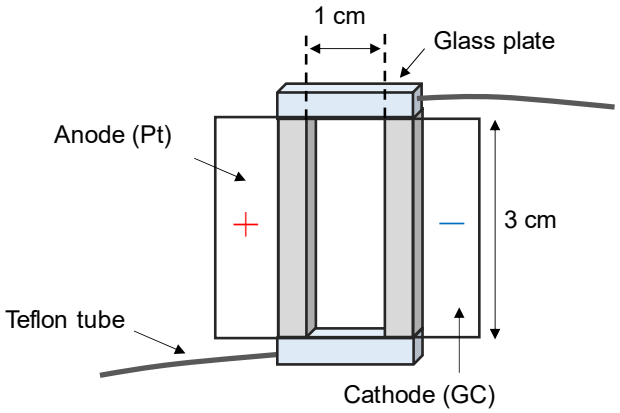

Fig. S1 Schematic of the electrochemical flow microreactor.

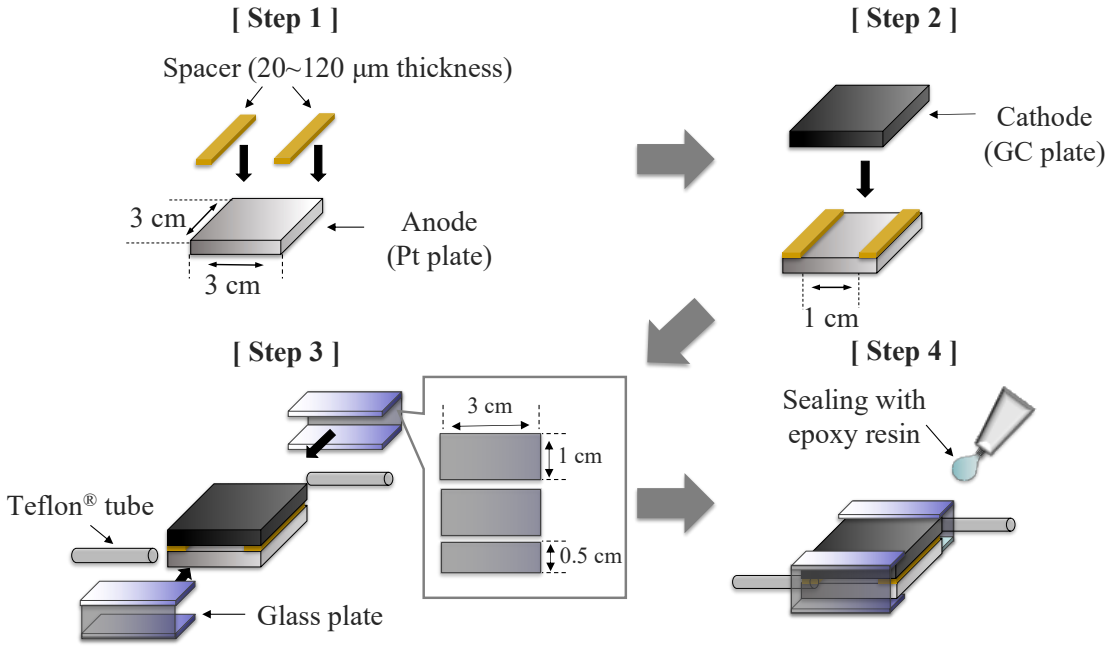

Fig. S2 Schematic of the construction procedure for the electrochemical flow microreactor.

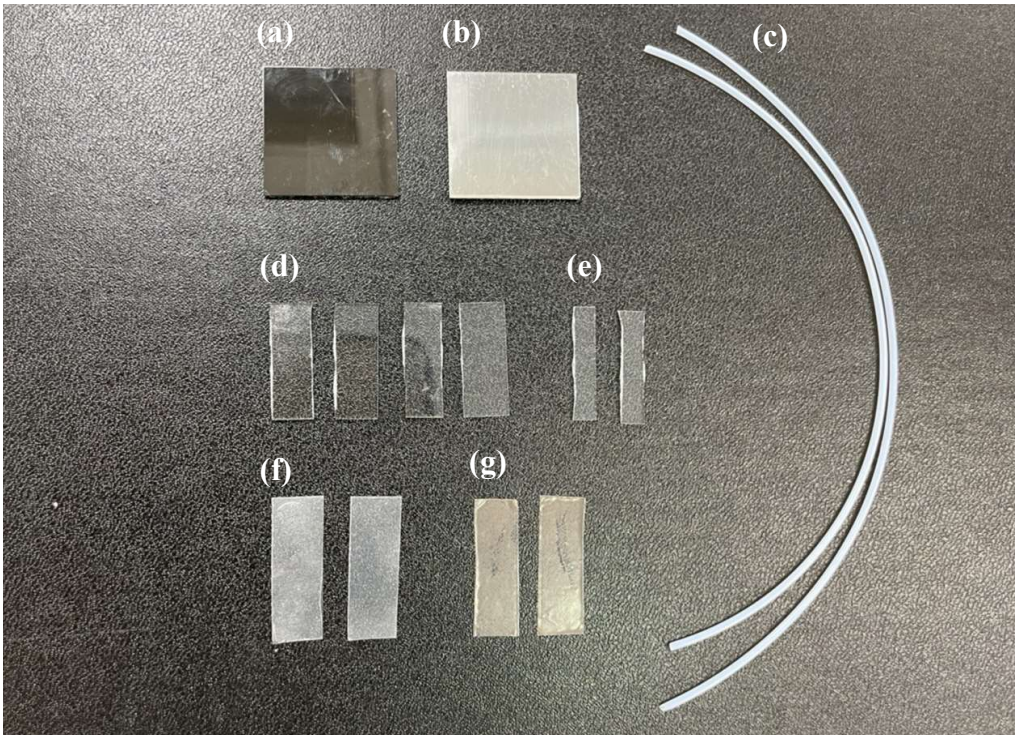

Fig. S3 Photograph of the parts used for the construction of microreactor. Alphabets in the figure corresponds to those in Table S1.

Table S1. List of parts used for the construction of microreactor

	Parts	Part numbers	Suppliers
(a)	GC plate (3 cm × 3 cm)	1	Tokai carbon
(b)	Pt plate1(3 cm × 3 cm)	1	Tokuriki Honten
(c)	Teflon tube	2	GL Sciences
(d)	Glass plate (1 cm × 3 cm)	4	Matsunami
(e)	Glass plate (0.5 cm × 3 cm)	2	Matsunami
(f)	Double-faced adhesive type (10 μm)	Depends	Nitto
(g)	Double-faced adhesive type (80 μm)	Depends	Nitto

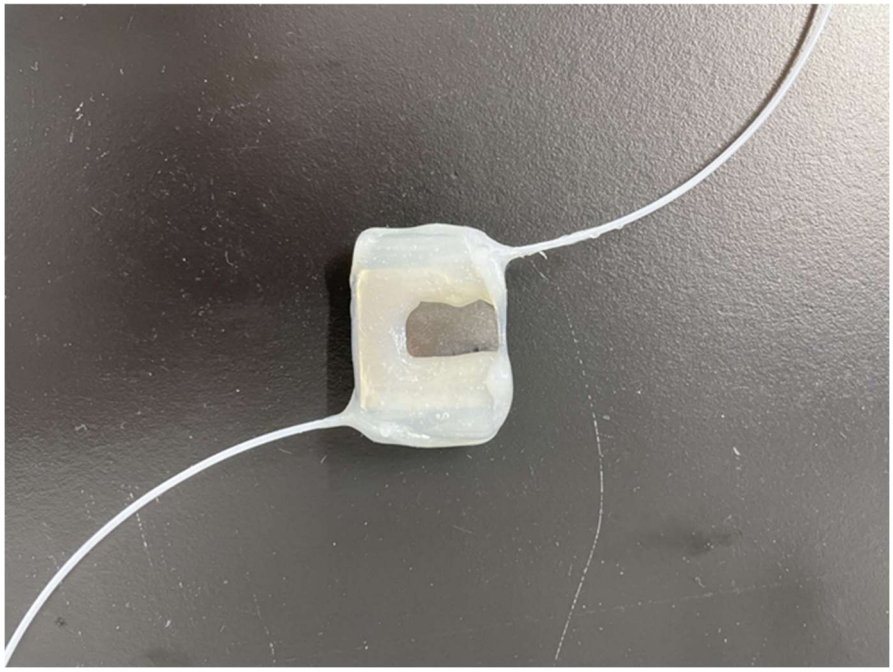

Fig. S4 Photograph of a flow microreactor.

4. General procedure for electrochemical carboxylation in electrochemical flow microreactor

The flow microreactor system for the model synthetic reaction was fabricated as illustrated in Fig. 1. The electrochemical carboxylation reaction was carried out by introducing a solution (Bu_4NClO_4 in tetrahydrofuran (THF)) containing an imine **1** and CO_2 via a syringe pump. The CO_2 solution was prepared by sparging CO_2 gas into THF for 30 min. The solution was then introduced into the electrochemical flow microreactor. At the cathode in the flow microreactor, imines were reduced and reacted with CO_2 to produce the corresponding carboxylate anions. In addition, THF was oxidized at the anode of the counter electrode to generate protons, as shown in Fig. 3e of the main text. The carboxylate anions were protonated by the protons generated at the anode, and amino acids were obtained. After electrolysis, 0.5 mL of each solution was collected with 1 M HCl aq. to confirm that all the carboxylates were protonated to produce amino acids. Each electrolyzed solution was diluted 20-fold and quantitatively analyzed by HPLC to determine the yield of α-amino acids. The calibration curves of α-amino acids **2a**–**f** in HPLC analysis were prepared using the corresponding authentic samples (see Fig. S16–21).

$$\text{Electricity } [\text{F mol}^{-1}] = \frac{\text{Passing charge in microreactor per second } [\text{F s}^{-1}]}{\text{Substrate introduced into microreactor per second } [\text{mol s}^{-1}]}$$

$$= \frac{\frac{1}{96{,}485}[\text{F C}^{-1}] \times \left(\text{Current density } [\text{mA cm}^{-2}] \times \frac{1}{1000}[\text{A mA}^{-1}] \times \text{Electrode surface area } [\text{cm}^2]\right)\ [\text{C s}^{-1}]}{\left(\text{flow rate } [\text{mL h}^{-1}] \times \frac{1}{1000}[\text{L mL}^{-1}] \times \frac{1}{3600}[\text{h s}^{-1}] \times \text{Concentration of substrate } [\text{mol L}^{-1}]\right)\ [\text{mol s}^{-1}]}$$

5. Concentration of CO_2 in THF

Concentrations of CO_2 in THF were determined by gas chromatography analysis. A gas chromatography calibration curve for the quantification of CO_2 was constructed using gaseous CO_2, where the volume was converted to molar units using the gas constant. THF solutions with solubilized CO_2 were prepared by bubbling CO_2 gas for various durations (1–30 min) under atmospheric pressure. Quantification of CO_2 was then performed by gas chromatography analysis (Fig. S5). The results showed that CO_2 was dissolved in THF to a concentration of 0.33 M after 30 min of bubbling. This concentration was sufficient for the concentration of the substrate investigated in the present work.

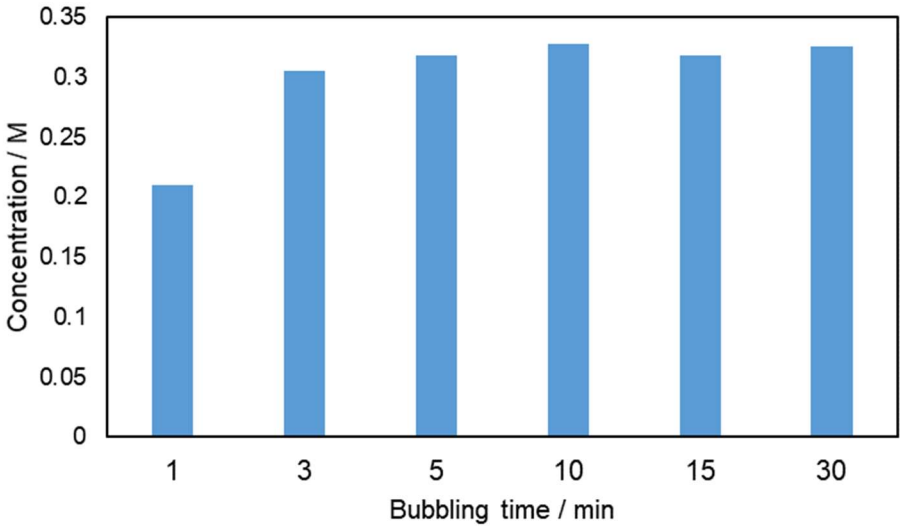

Fig. S5 Concentration of CO_2 solubilized in THF as a function the bubbling time.

6. Script for Bayesian optimization

Constrained Bayesian optimization using GPyOpt for Entries 6A–9A in Table 1 and Table S2

```
import numpy as np
import GPy, GPyOpt
```

```
X = np.array([[0.08, 0.1, 25., 15., 120.],
              [0.08, 0.15, 40., 25., 80.],
              [0.04, 0.1, 10., 10., 20.],
              [0.04, 0.05, 25., 25., 120.],
              [0.12, 0.15, 15., 5., 80.],
             [0.049, 0.1, 11.1, 8.9, 30.],
             [0.062, 0.075, 12.2, 7.4, 20.],
             [0.045, 0.12, 10.1, 9.2, 30.],
             [0.043, 0.077, 11.9, 11.1, 30.]])

Y = np.array([28., 31., 88., 39., 46., 90., 78., 78., 81.])[:, np.newaxis]

bounds = [{'name': '[1a]', 'type': 'continuous', 'domain': (0.04,0.12)},
          {'name': '[electrolyte]', 'type': 'continuous', 'domain': (0.05,0.15)},
          {'name': 'current density', 'type': 'continuous', 'domain': (10,40)},
          {'name': 'flow rate', 'type': 'continuous', 'domain': (5,25)},
          {'name': 'electrode distance', 'type': 'continuous', 'domain': (20,120)}
         ]
```

```
constraints = [{'name': 'constr_1', 'constraint': '2 - (0.112 * x[:,2]) / (x[:,0] * x[:,3])'},
               {'name': 'constr_2', 'constraint': '(0.112 * x[:,2]) / (x[:,0] * x[:,3]) - 3'}]
```

```
myBopt = GPyOpt.methods.BayesianOptimization(f=None,
                                             domain=bounds,
                                             constraints=constraints,
                                             X = X,
                                             Y = Y,
                                             acquisition_type='EI',
                                             )

next_x = myBopt.suggest_next_locations()
print(next_x)
```

Constrained Bayesian optimization using GPyOpt for Entries 6B–9B in Table 1 and Table S2

```
import numpy as np
import GPy, GPyOpt
```

```
X = np.array([[0.08, 0.1, 25., 15., 120.],
              [0.08, 0.15, 40., 25., 80.],
              [0.04, 0.1, 10., 10., 20.],
              [0.04, 0.05, 25., 25., 120.],
              [0.12, 0.15, 15., 5., 80.],
             [0.04, 0.084, 10.6, 14.6, 30.],
             [0.071, 0.053, 10.6, 8.3, 40.],
             [0.06, 0.15, 11.7, 10.8, 20.],
             [0.042, 0.094, 12.2, 16., 20.]])

Y = np.array([28., 31., 88., 39., 85., 71., 77., 88.])[:, np.newaxis]

bounds = [{'name': '[1a]', 'type': 'continuous', 'domain': (0.04,0.12)},
          {'name': '[electrolyte]', 'type': 'continuous', 'domain': (0.05,0.15)},
          {'name': 'current density', 'type': 'continuous', 'domain': (10,40)},
          {'name': 'flow rate', 'type': 'continuous', 'domain': (5,25)},
          {'name': 'electrode distance', 'type': 'continuous', 'domain': (20,120)}
         ]
```

```
constraints = [{'name': 'constr_1', 'constraint': '2 - (0.112 * x[:,2]) / (x[:,0] * x[:,3])'},
           {'name': 'constr_2', 'constraint': '(0.112 * x[:,2]) / (x[:,0] * x[:,3]) - 2.1'}]
```

```
myBopt = GPyOpt.methods.BayesianOptimization(f=None,
                                             domain=bounds,
                                             constraints=constraints,
                                             X = X,
                                             Y = Y,
                                             acquisition_type='EI',
                                             )

next_x = myBopt.suggest_next_locations()
print(next_x)
```

7. Complete experimental conditions and experimental results for Bayesian optimization

Table S2 shows the complete experimental conditions and the corresponding electrolysis results for the Bayesian optimization (BO) cycles. The yield of **1a** was evaluated by sampling 0.5 mL of a fraction from the outlet of the microreactor. Four fractions were sequentially collected for determination of the yield, and the yield for the 1st fraction was used as training data for BO. Entries with uppercase letters represent sets of conditions suggested by the BO, where "A" and "B" indicate BOs performed under constraints "$2.0 < q < 3.0$" and "$2.0 < q < 2.1$", respectively (where q denotes the passed charge, F mol^{-1}). Our BO algorithm suggests one candidate from many maxima in an acquisition function. This system occasionally suggests almost the same conditions as those in the initial dataset as well as harsh conditions that would damage the reactor. In such cases, new parameters recalculated by the BO algorithm were used for the optimization. The yield of **1a** was added as new training data, followed by another BO. Following this cycle, BOs and experiments were performed in numerical order after 6A and 6B (Table S2).

Table S2. Complete experimental conditions and experimental results calculated by Bayesian optimization

	Entry	[1a] / M	[Bu_4NClO_4] / M	Current density / mA cm^{-2}	Flow rate / mL h^{-1}	Electrode distance / μm	Charge Passed (q) / F mol^{-1}	Yield of 2a[b] for collected fraction/ % 1st	2nd	3rd	4th
Training data	1	0.08	0.1	25	15	120	2.33	28	30	35	31
	2	0.08	0.15	40	25	80	2.24	31	38	38	42
	3	0.04	0.1	10	10	20	2.80	88	62	54	1
	4	0.04	0.05	25	25	120	2.80	39	38	39	0
	5	0.12	0.15	15	5	80	2.80	46	49	45	×
2.0 < q < 3.0	6A	0.049	0.1	11.1	8.9	30	2.85	90	96	82	72
	7A	0.062	0.075	12.2	7.4	20	2.98	78	78	47	37
	8A	0.045	0.12	10.1	9.2	30	2.73	78	67	57	54
	9A	0.043	0.077	11.9	11.1	30	2.79	81	83	67	56
2.0 < q < 2.1	6B	0.04	0.084	10.6	14.6	30	2.03	85	82	73	72
	7B	0.071	0.053	10.6	8.3	40	2.01	71	63	59	49
	8B	0.06	0.15	11.7	10.8	20	2.02	77	70	63	61
	9B	0.042	0.094	12.2	16	20	2.03	88	85	78	55

[a]Reaction conditions: cathode, glassy carbon plate; anode, Pt plate; solvent, THF saturated with CO_2. [b]Determined by HPLC

8. Substrate scope for electrochemical carboxylation of imine derivatives

The scope of the substrate was examined to determine the optimum conditions. The conditions in Entry 9B in Table 1 were applied to the electrochemical carboxylation of various imines **1b–e**. Each electrolyzed solution was diluted 20-fold and quantitatively analyzed by HPLC to determine the yield of α-amino acids **2b**–**f**. α-Amino acids **2b–e** were obtained in reasonable yields. In a previous study, we reported the synthesis of **2b** from **1b** in 71% yield using Bu_4NClO_4/THF as an electrolyte in a flow microreactor.[8] Thus, ML-assisted optimization achieved a result similar to the optimized result achieved by a human. The relatively high yields for **2c–f** in our previous study (56–97% yields) was attributed to the difference in the supporting electrolyte, where a bulkier cation ($^nHex_4N^+$) was used to suppress ionic interaction with an imine-derived anionic intermediate. Notably, the ML-model in our study was constructed for the reaction of benzophenone imine **1a**, which is chemically inherently different from aldimine derivatives **1b–f**. Thus, some space exists to develop a better model for **1b–f**.

Table S3. Substrate scope for electrochemical carboxylation of imine derivatives **1b–f**[a]

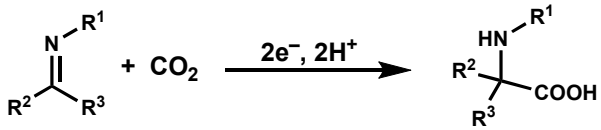

1b-f **2b-f**

Entry	Imine	R^1	R^2	R^3	Yield of α-amino acids **2**[b](%)
1	**1b**	Ph	Ph	H	60
2	**1c**	Ph	4-$MeOC_6H_4$	H	62
3	**1d**	4-$MeOC_6H_4$	Ph	H	69
4	**1e**	Ph	4-$CF_3C_6H_4$	H	61
5	**1f**	4-$CF_3C_6H_4$	Ph	H	37

[a]Reaction conditions: cathode, glassy carbon plate; anode, Pt plate; current density, 12.2 mA cm^{-2}; electrode distance, 20 μm; solvent, THF; concentration of CO_2, saturation concentration at 1 atm (~0.4 M, see ESI for details); [**1b–f**], 0.042 M; supporting electrolyte, 0.094 M Bu_4NClO_4; flow rate, 16 mL h^{-1}. [b]Determined by HPLC.

9. Visualization of BO-assisted multiparameter screening under the constraint 2.0 < *q* < 3.0

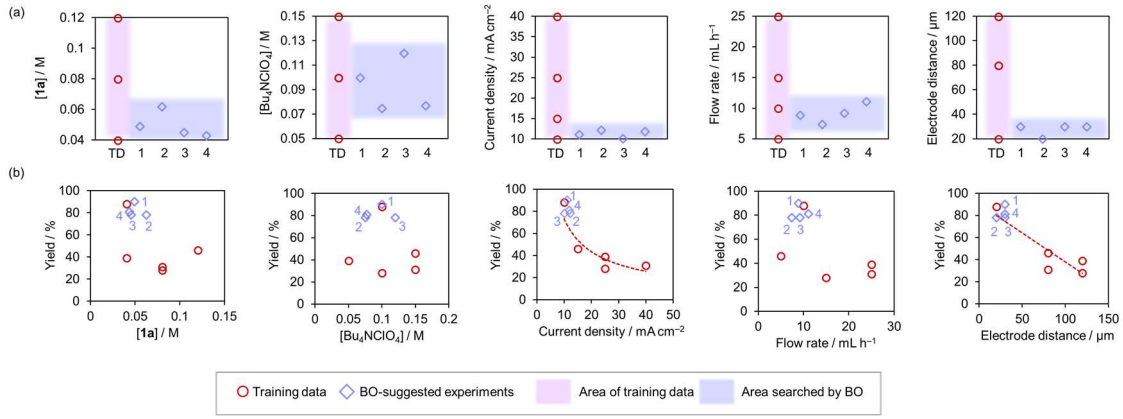

Fig. S6 Visualization of BO-assisted multiparameter screening under the constraint 2.0 < *q* < 3.0. (a) Plot of the experimental parameters as a function of the number of BO cycles. The number of BO cycles (1 to 4) is shown on the horizontal axes. Regions highlighted by red and blue represent the area of the training dataset and the area searched by BO, respectively. (b) Plot of the experimental parameters as a function of the yields of **2a** with different constraints on passed charge. The numbers in the plots in (b) indicate the correspondence with the number of BO cycles (1 to 4). The training dataset (TD) and datasets for BO-suggested experiments are represented as red circles and pale-blue diamonds, respectively.

10. Establishing relationship between $I_{lim,diffusion}$ and I_{BE}

The diffusion-controlled limiting current ($I_{lim,diffusion}$) is a faradaic current that is independent of the applied potential; it is observed under conditions where the supply of a reaction substrate onto the electrode surface is limited. The $I_{lim,diffusion}$ is experimentally observed as a plateau in the current–voltage (I–V) curve. The theoretical representation of $I_{lim,diffusion}$ for a rectangular channel flow configuration is established as Eq. S1 under the constraint that the bulk concentration of the substrate is constant, i.e., the consumption of the substrate by the electrochemical reaction is sufficiently small.[9,10]

$$I_{\mathrm{lim,diffusion}} = 0.925nFc\left(\frac{DA}{h}\right)^{\frac{2}{3}}(V_{\mathrm{f}})^{\frac{1}{3}} \qquad \text{Eq. S1}$$

where n is the number of electrons transferred from/to a molecule of interest, F is the Faraday constant (96,485 C mol^{-1}), c is the bulk concentration of the substrate, D is the diffusion coefficient for the substrate, A is the electrode area, V_f is the volume flow rate, and h is the half-height of the gap distance of the electrodes. However, under the electrolytic condition, the electrochemical reaction (i.e., the consumption of the substrate of interest) is more pronounced; thus, the $I_{lim,diffusion}$ value no longer follows Eq. S1. Hence, in this section, we aimed to establish a qualitative description of $I_{lim,diffusion}$ under electrolytic conditions as well as its relationship with I_{BE}.

Here, we consider a steady-state electrolysis reaction in a continuous flow system under diffusion-controlled conditions. The electrochemical reaction rate is determined by mass transfer toward the electrode. The Faraday constant (96,485 C mol^{-1}) can be used to convert the limiting current (I_{lim} [A] = [C s^{-1}]) to the rate of electron transfer at the electrode surface (mol(electron) s^{-1}), consistent with the mass transfer rate of the substrate to the electrode surface (mol(substrate) s^{-1}, here represented as v_1) multiplied by n (number of electrons transferred per substrate), as shown in Eq. S2 (Fig. S7):

$$I_{\mathrm{lim,diffusion}} = nv_1 \qquad \text{Eq. S2}$$

However, the current for full conversion of a substrate is defined as I_{BE} (where BE represents bulk electrolysis; the details of the definition of I_{BE} are given in the main text). I_{BE} is determined as the product of the concentration (c) of the substrate in the electrolyte before it is introduced into the flow microreactor and the volume flow rate (v) of the electrolyte. Therefore, I_{BE} is equal to the rate of introduction of the substrate into the flow microreactor

(mol(substrate) s^{-1}, here represented as v_2):

$$I_{BE} = nv_2 \qquad \text{Eq. S3}$$

Notably, v_1 never exceeds v_2 because the amount of substrate near the electrode surface (v_1t, where t represents time) is a portion of the total amount of substrate introduced into the reactor (v_2t):

$$v_1 \leqq v_2 \qquad \text{Eq. S4}$$

From Eqs. S2–S4, Eq. S5 is established:

$$I_{lim} \leqq I_{BE} \qquad \text{Eq. S5}$$

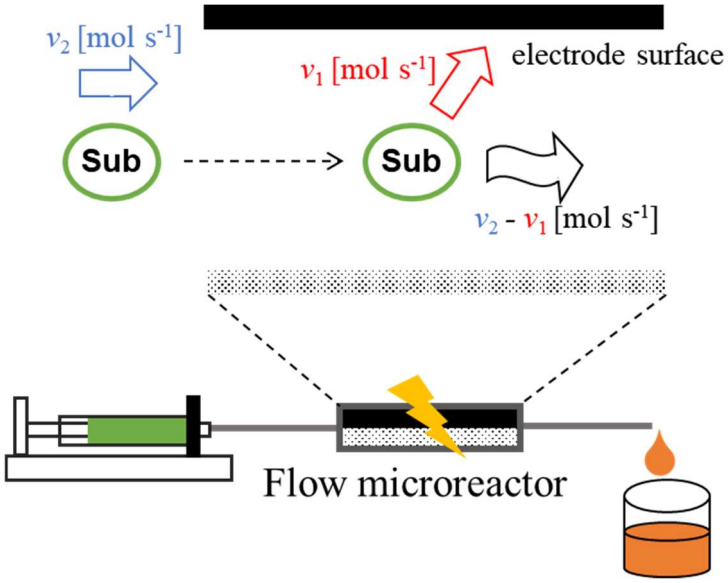

Fig. S7 Schematic of the mass transfer rate of the substrate to the electrode surface (v_1) versus the introduction rate of the substrate into the flow microreactor (v_2).

11. Linear sweep voltammetry and chronoamperometry

To evaluate $I_{lim,diffusion}$ under the conditions specified in Entry 9B of Table 1, a linear sweep voltammetry (LSV) measurement was first performed. Fig. S8 shows the resultant voltammogram, where a plateau was faintly observed at approximately −1.6 V (blue area).

To precisely determine the $I_{lim,diffusion}$ value, steady-state currents were measured using a chronoamperometric technique in a flow microreactor under the same conditions (Fig. S9). Fig. 3d in the manuscript was constructed using the $I_{lim,diffusion}$ values at each potential in Fig. S9.

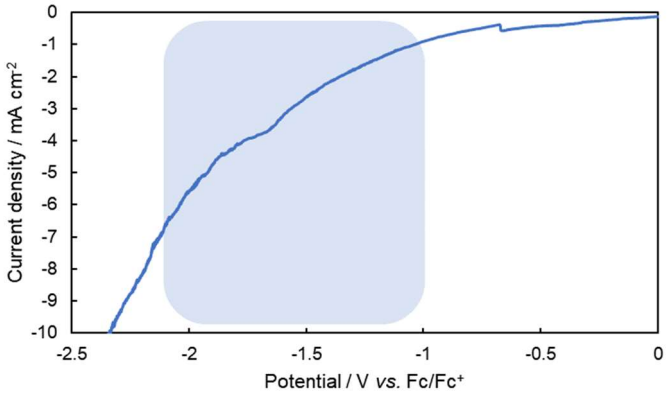

Fig. S8 Linear sweep voltammograms recorded in a flow microreactor. Experimental conditions: cathode; GC plate, anode; Pt plate, reference electrode; Ag wire, substrate **1a**; 0.042 M, supporting electrolyte Bu_4NClO_4; 0.094 M, flow rate; 16 mL h^{-1}, electrode distance; 20 μm, solvent; THF saturated with CO_2.

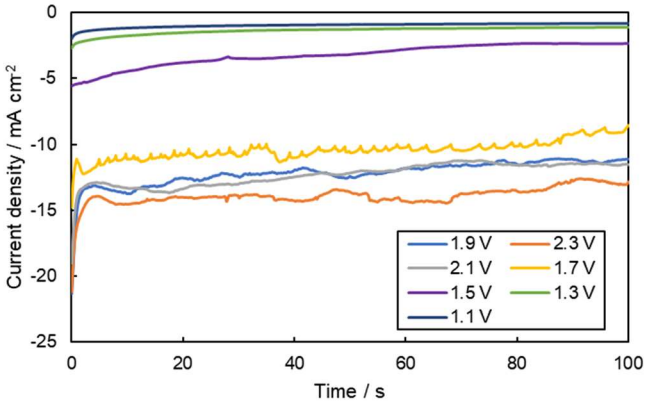

Fig. S9 Chronoamperometry measurements in a flow microreactor. Experimental conditions: cathode; GC plate, anode; Pt plate, reference electrode; Ag wire, substrate **1a**; 0.042 M, supporting electrolyte Bu_4NClO_4; 0.094 M, flow rate; 16 mL h^{-1}, electrode distance; 20 μm, solvent; THF saturated with CO_2.

12. HPLC analysis

Typical examples of HPLC charts and calibration curves for HPLC analysis are presented here.

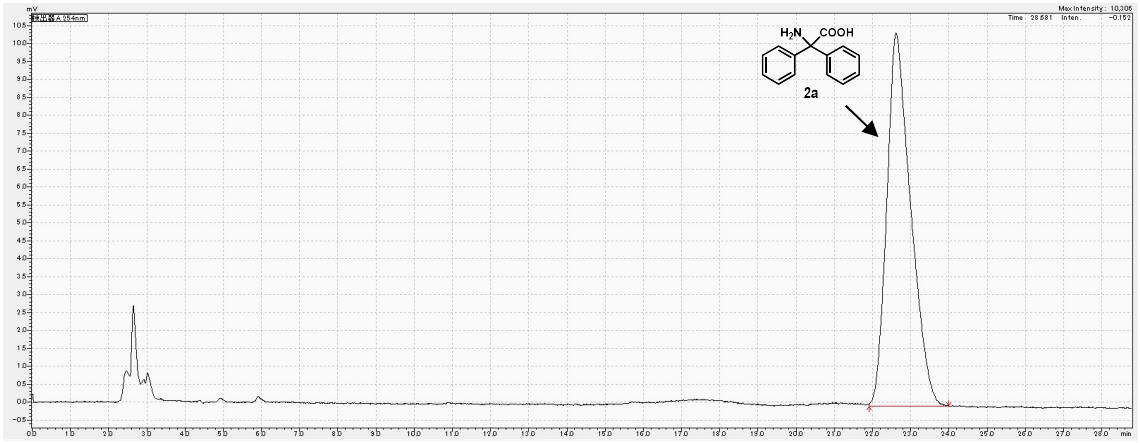

Fig. S10 HPLC chart of the reaction mixture obtained after electrochemical carboxylation of **1a** (corresponding to Entry 9B (fraction 2) in Table S2).

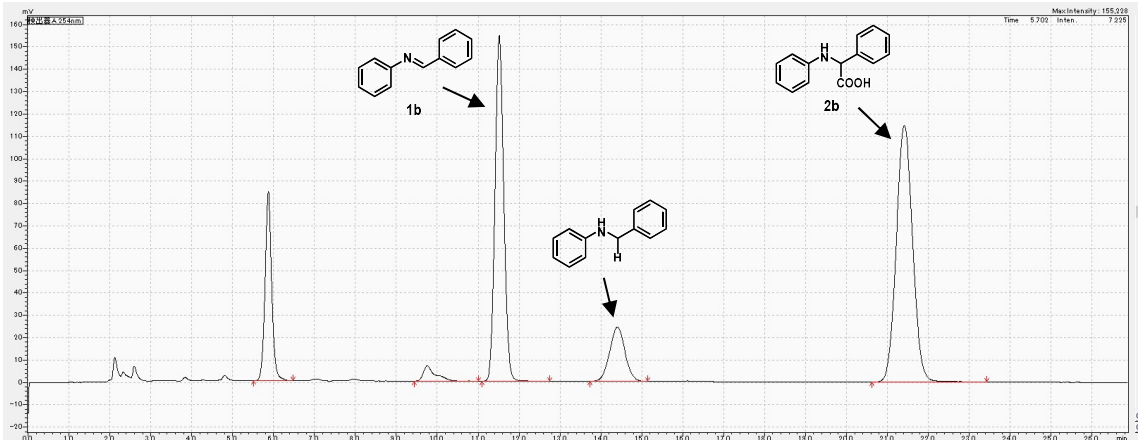

Fig. S11 HPLC chart of the reaction mixture obtained after electrochemical carboxylation of **1b**.

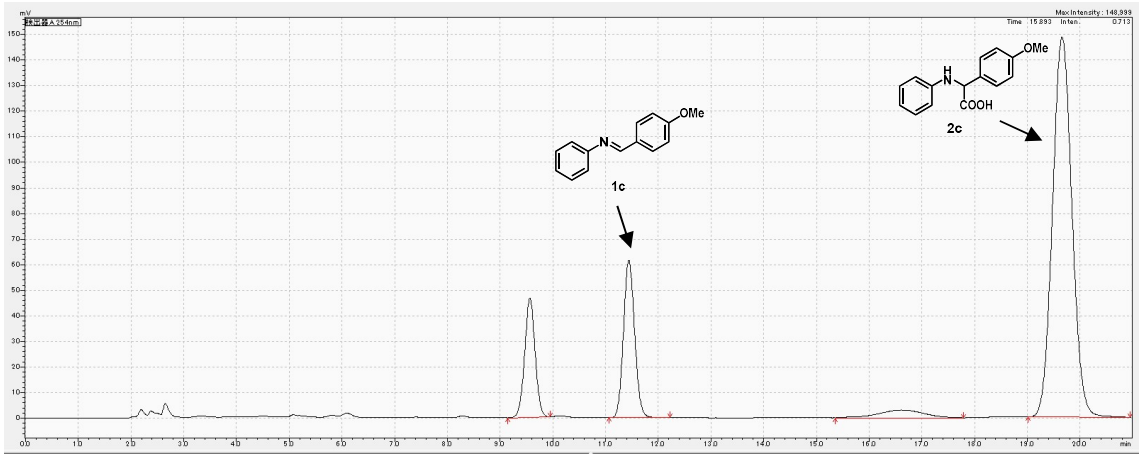

Fig. S12 HPLC chart of the reaction mixture obtained after electrochemical carboxylation of **1c**.

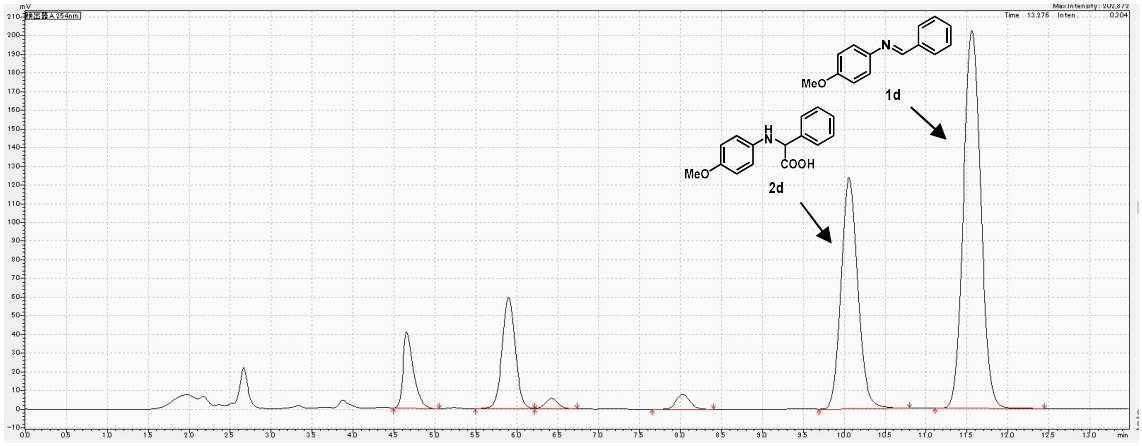

Fig. S13 HPLC chart of the reaction mixture obtained after electrochemical carboxylation of **1d**.

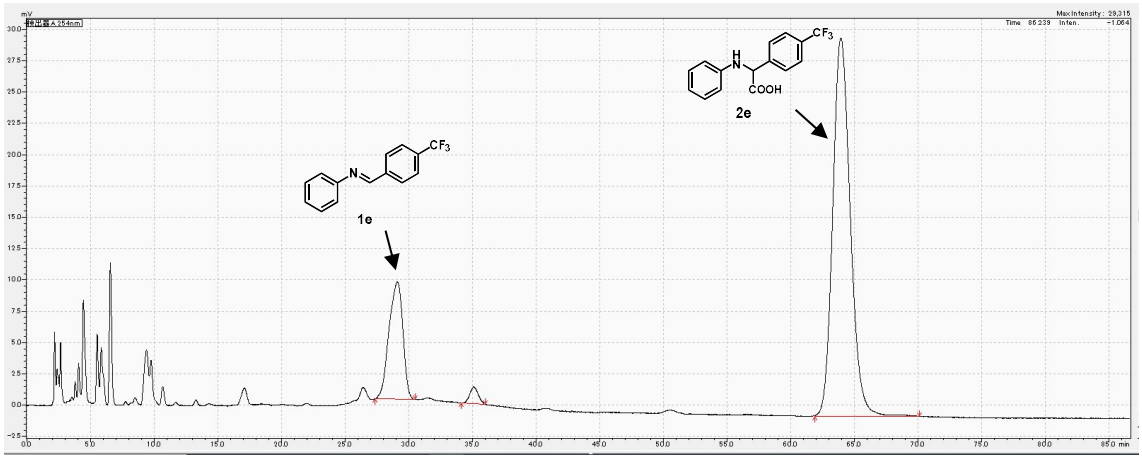

Fig. S14 HPLC chart of the reaction mixture obtained after electrochemical carboxylation of **1e**.

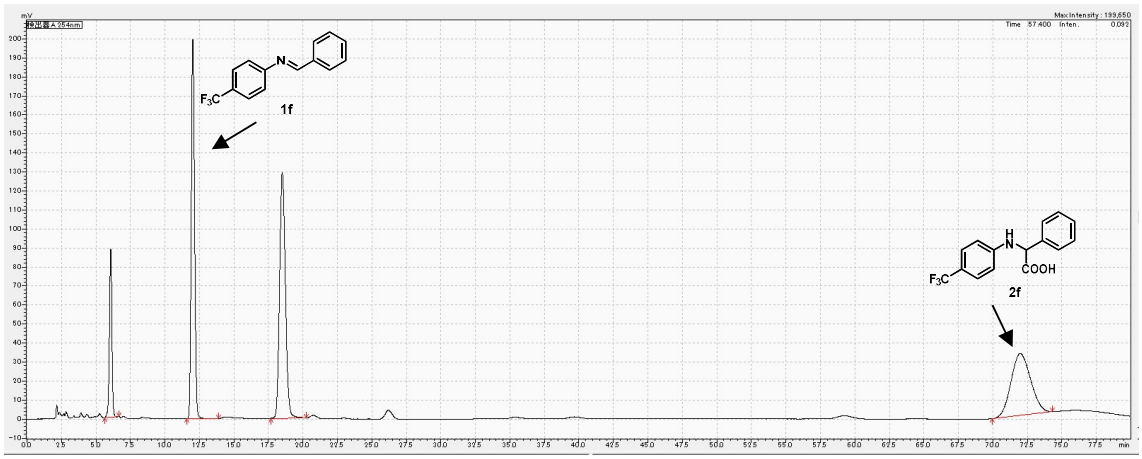

Fig. S15 HPLC chart of the reaction mixture obtained after electrochemical carboxylation of **1f**.

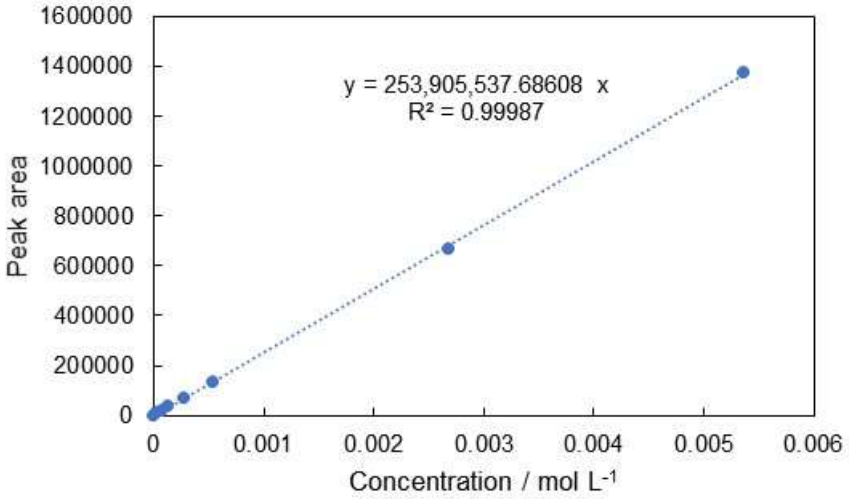

Fig. S16 Calibration curve for **2a** for HPLC analysis.

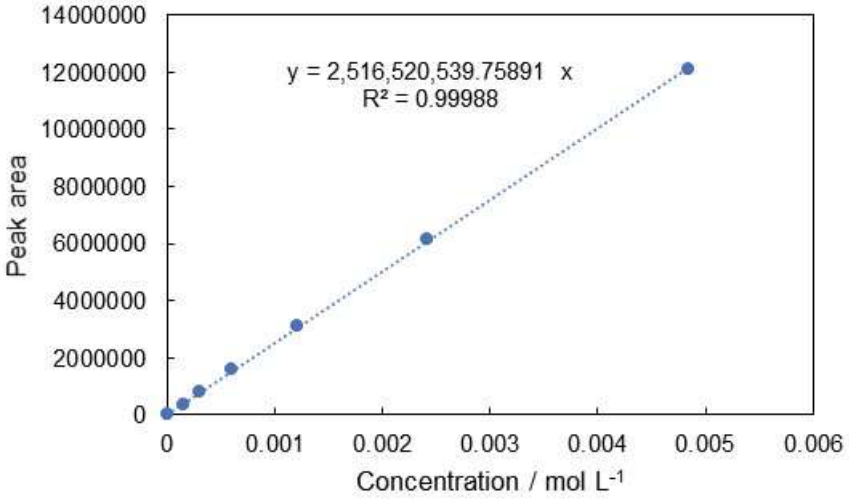

Fig. S17 Calibration curve for **2b** for HPLC analysis.

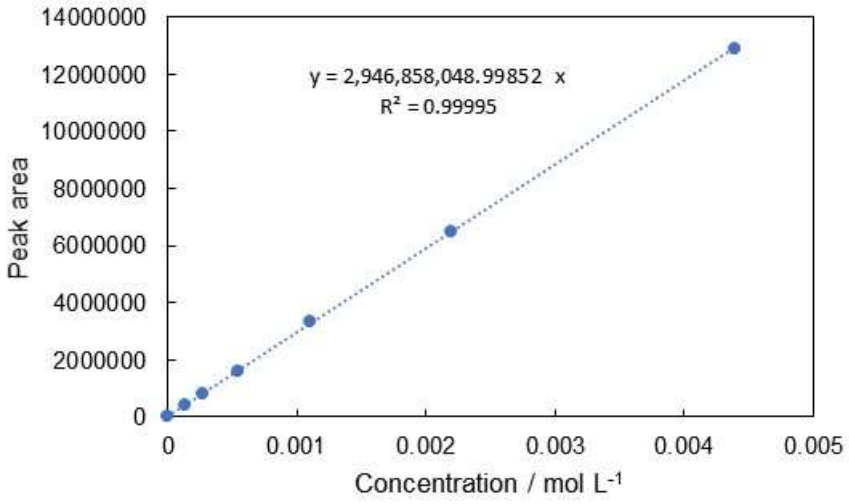

Fig. S18 Calibration curve for **2c** for HPLC analysis.

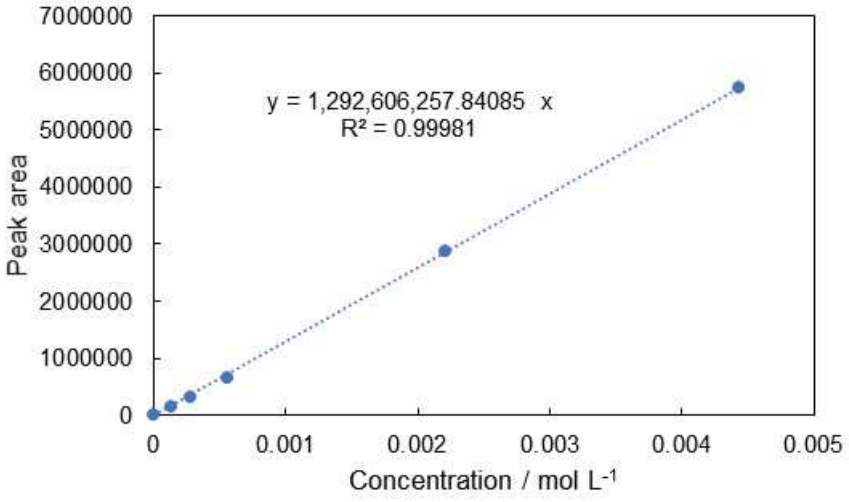

Fig. S19 Calibration curve for **2d** for HPLC analysis.

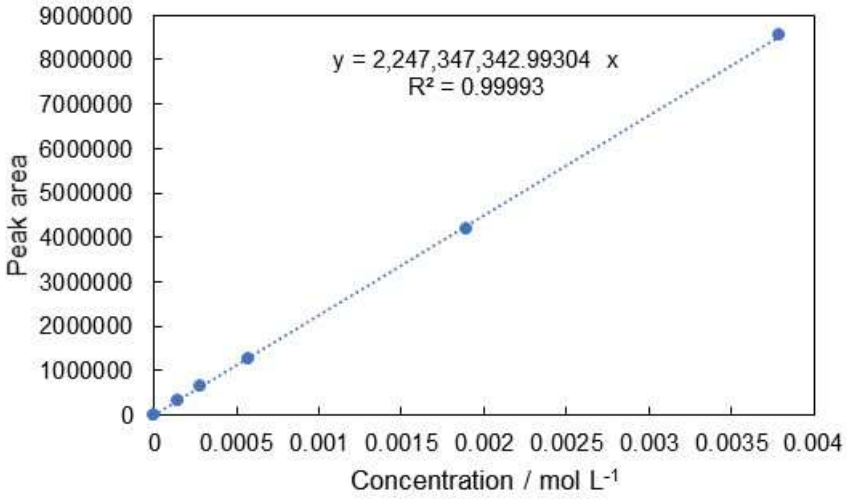

Fig. S20 Calibration curve for **2e** for HPLC analysis.

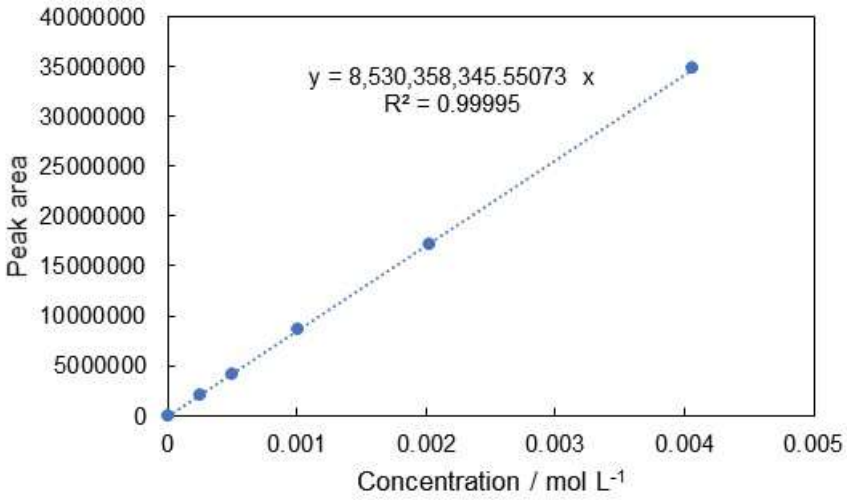

Fig. S21 Calibration curve for **2f** for HPLC analysis.

13. Gas chromatography analysis

Gas chromatography analyses were performed to determine the concentration of CO_2 dissolved in THF.

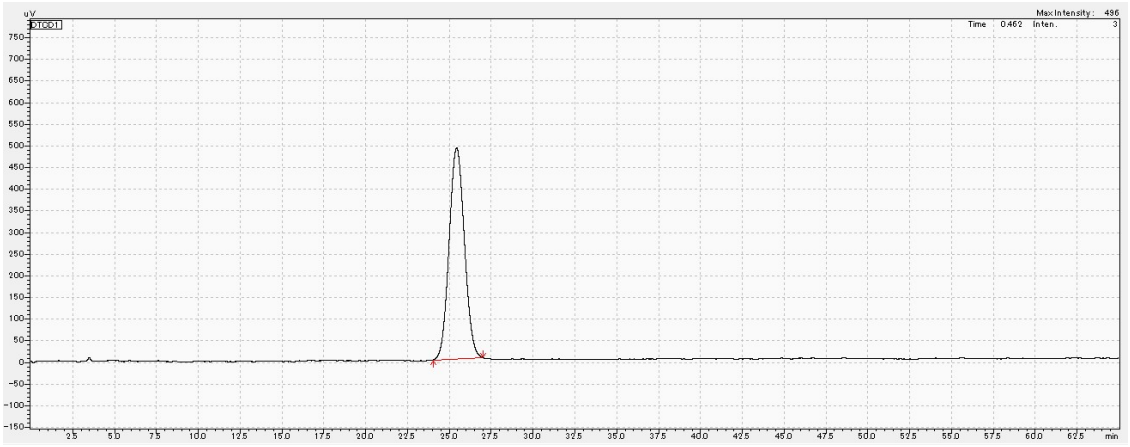

Fig. S22 Gas chromatogram of THF saturated with CO_2.

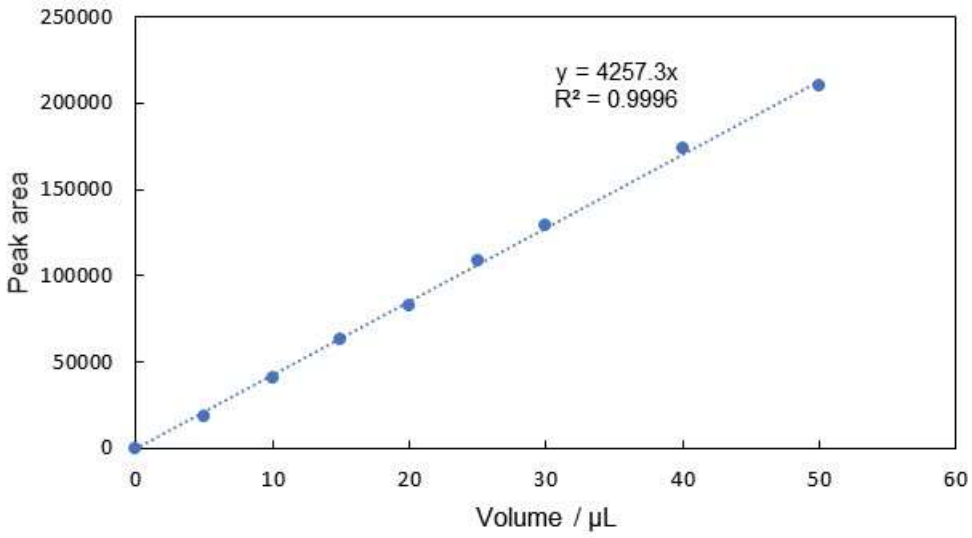

Fig. S23 Calibration curve for CO_2 for gas chromatography analysis.

14. ^{1}H NMR spectra

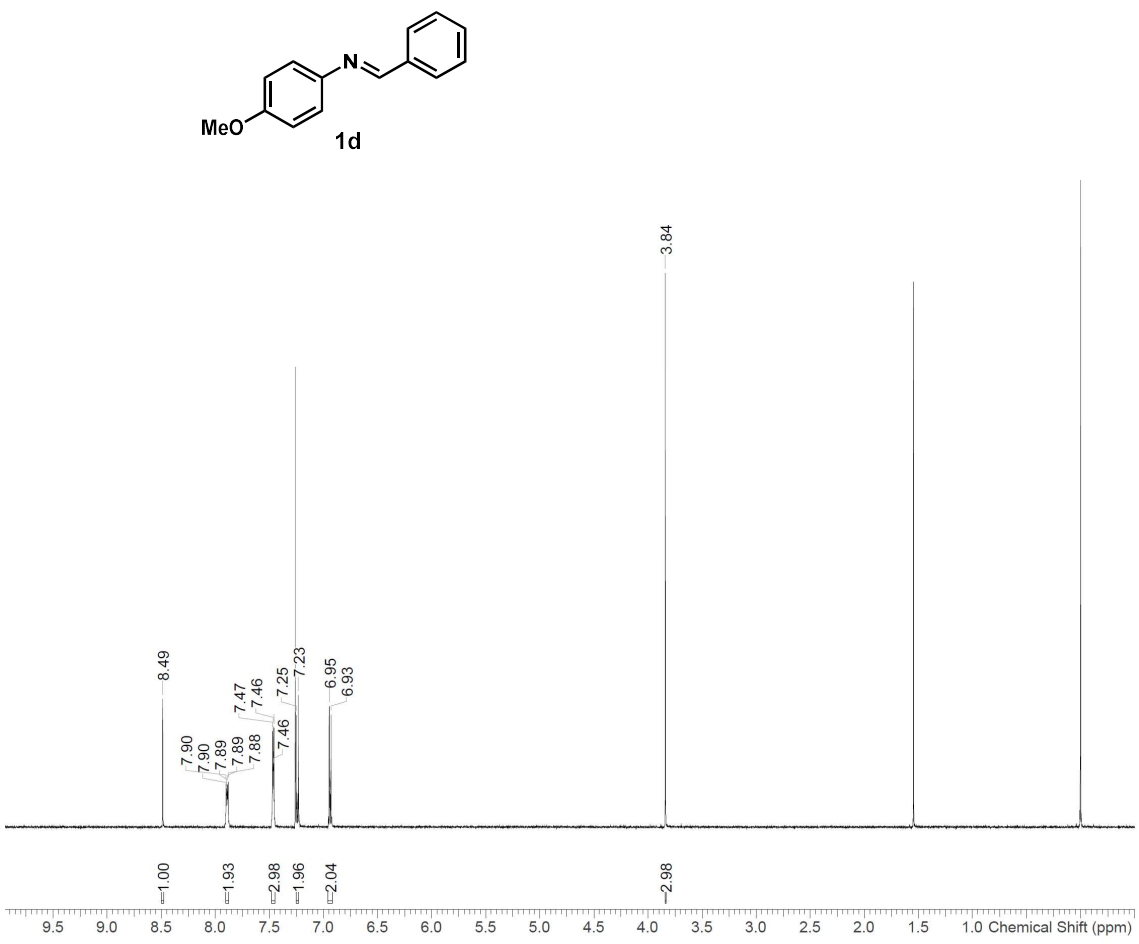

Fig. S24 ^{1}H NMR (500 MHz; $CDCl_3$) spectrum of *N*-benzylidene-4-methoxyaniline (**1d**).

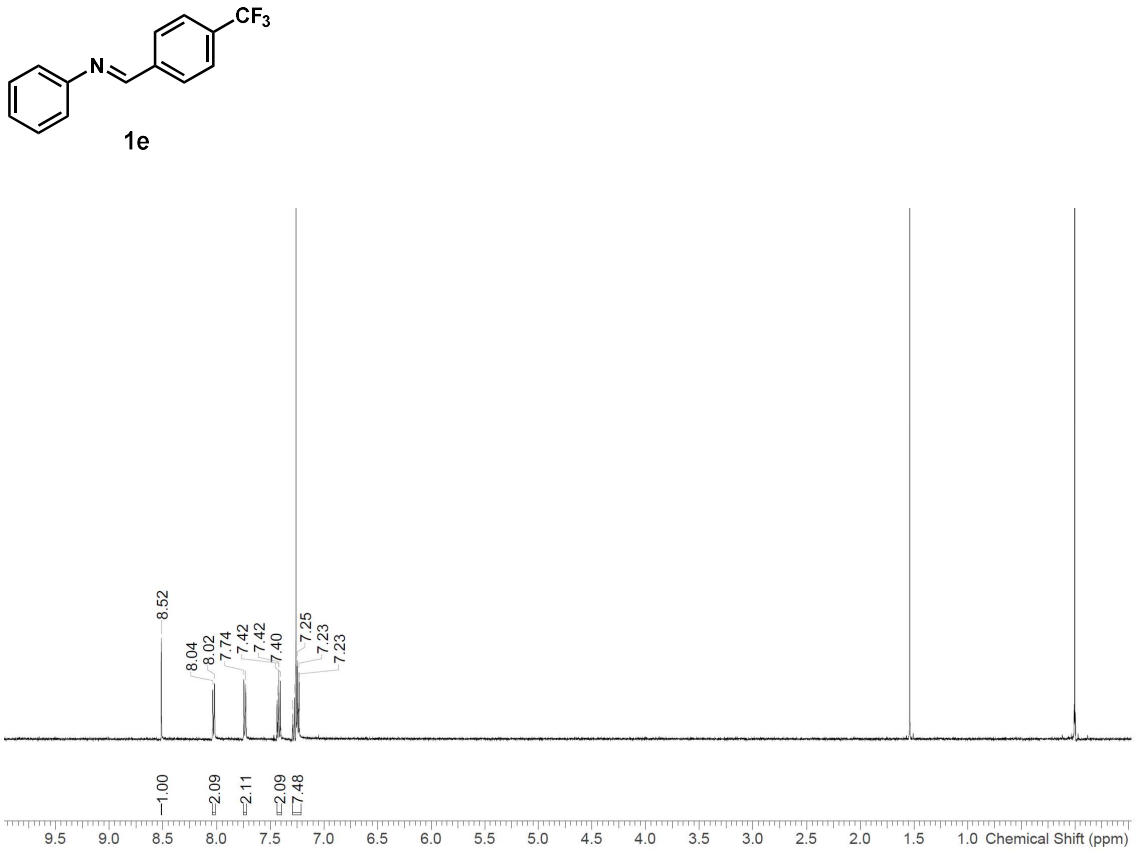

Fig. S25 ^{1}H NMR (500 MHz; $CDCl_3$) spectrum of *N*-(4-(trifluoromethyl)benzylidene)aniline (**1e**).

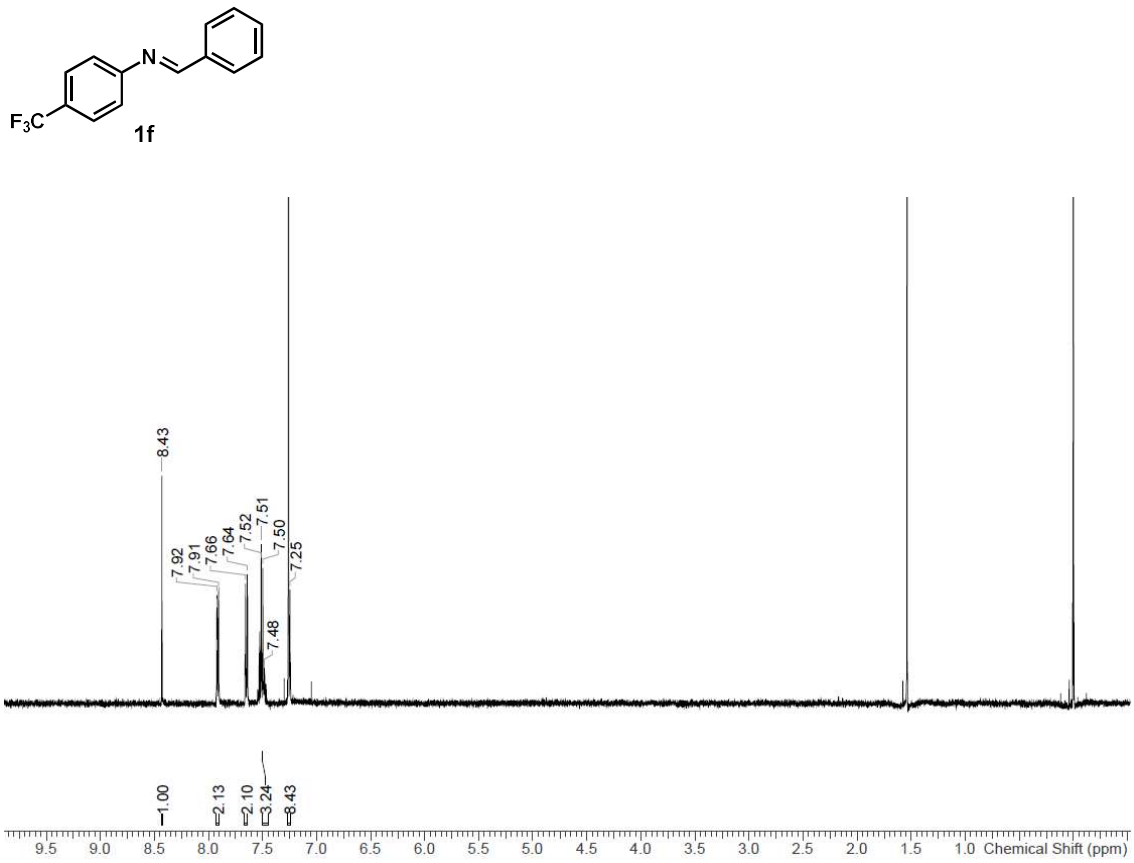

Fig. S26 ^{1}H NMR (500 MHz; $CDCl_3$) spectrum of *N*-benzylidene-4-trifluoromethylaniline (**1f**).

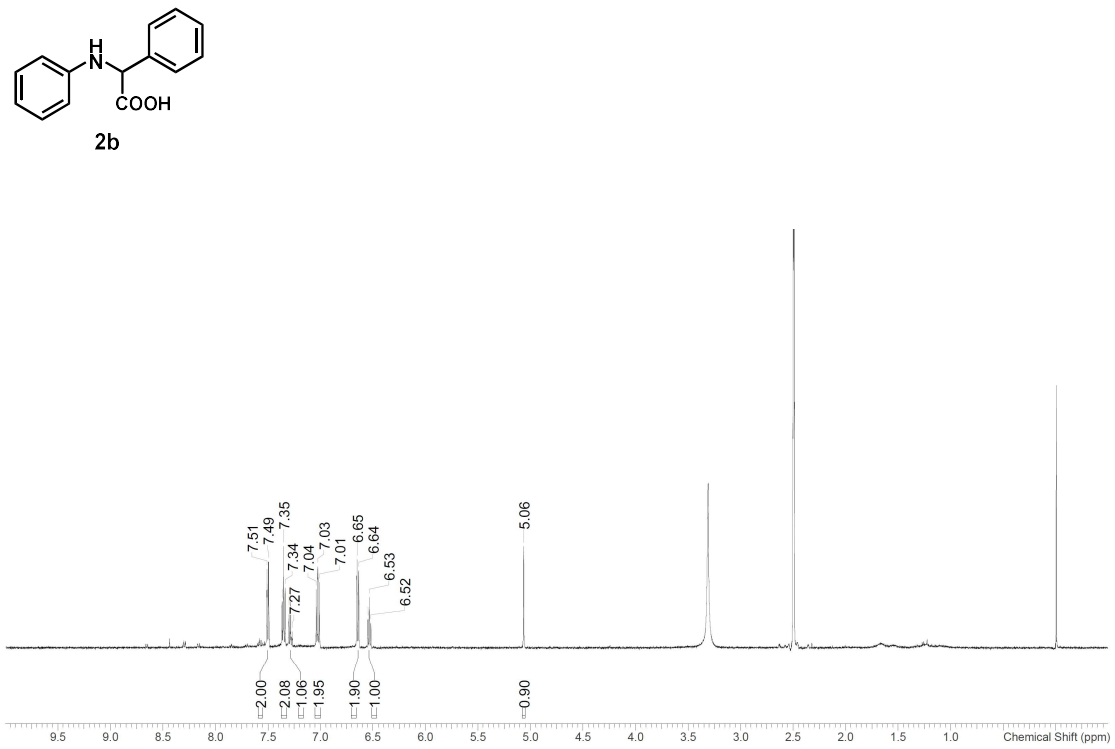

Fig. S27 ^{1}H NMR (500 MHz, DMSO-d_6) spectrum of α-(phenylamino)-benzeneacetic acid (**2b**).

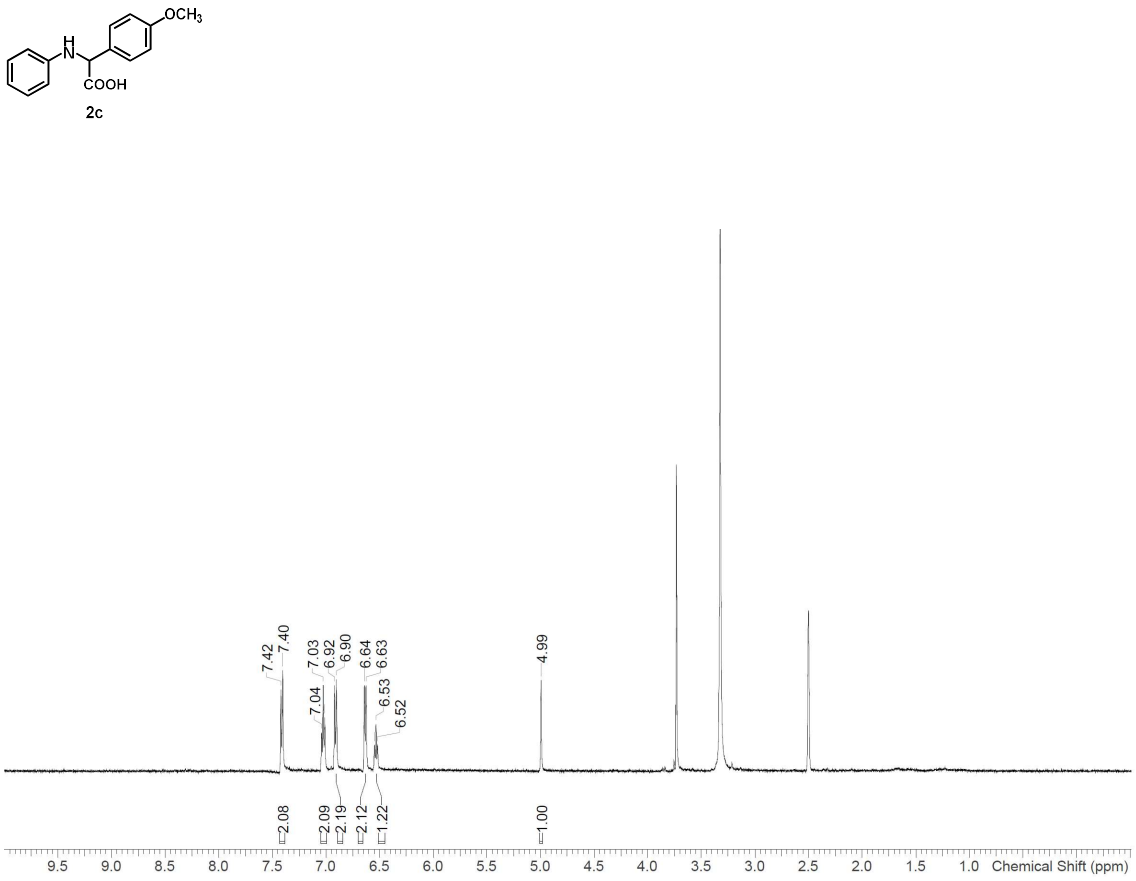

Fig. S28 ^{1}H NMR (500 MHz, DMSO-d_6) spectrum of 4-methoxy-α-(phenylamino)-benzeneacetic acid (**2c**).

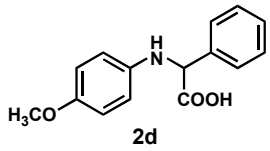

2d

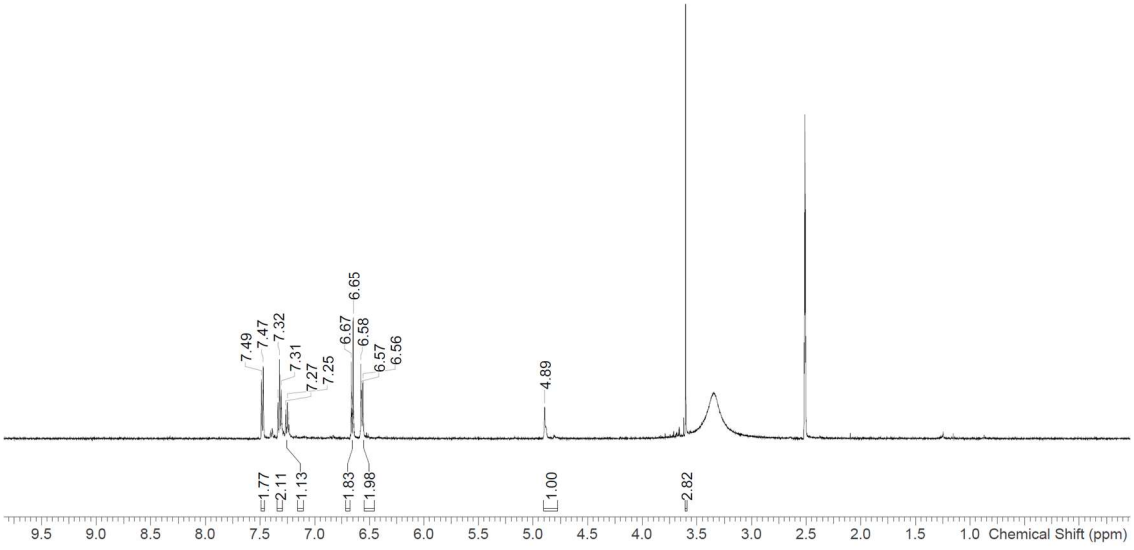

Fig. S29 ^{1}H NMR (500 MHz, DMSO-d_6) spectrum of α-[(4-methoxyphenyl)amino]-benzeneacetic acid (**2d**).

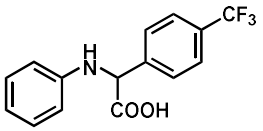

2e

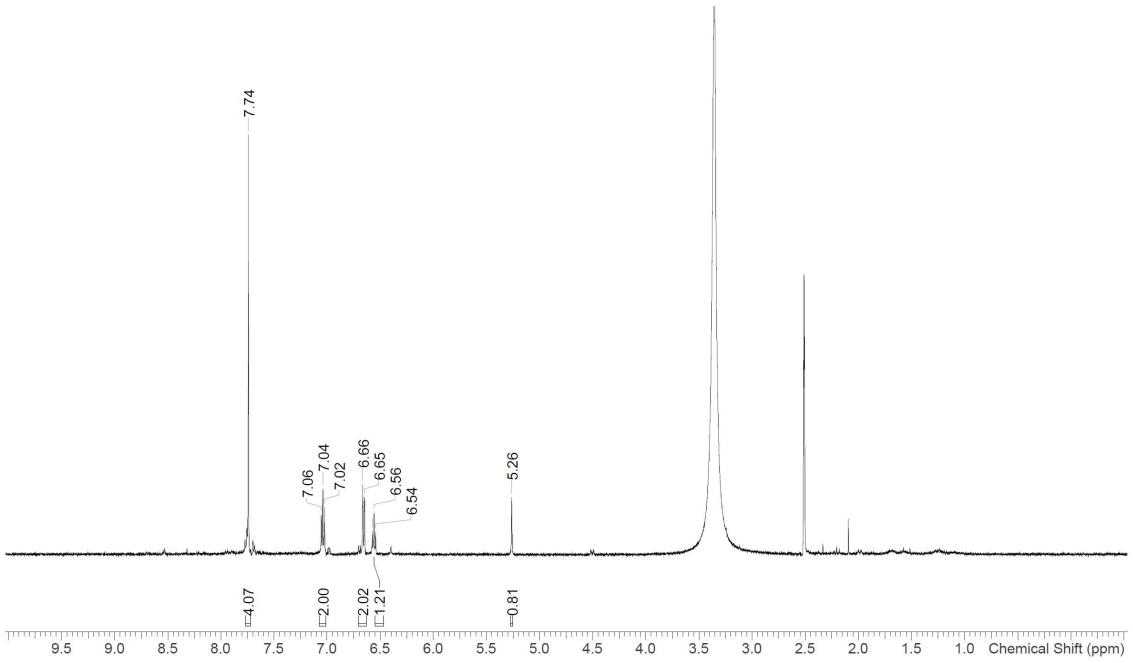

Fig. S30 ^{1}H NMR (500 MHz, DMSO-d_6) spectrum of α-(phenylamino)-4-(trifluoromethyl)-benzeneacetic acid (**2e**).

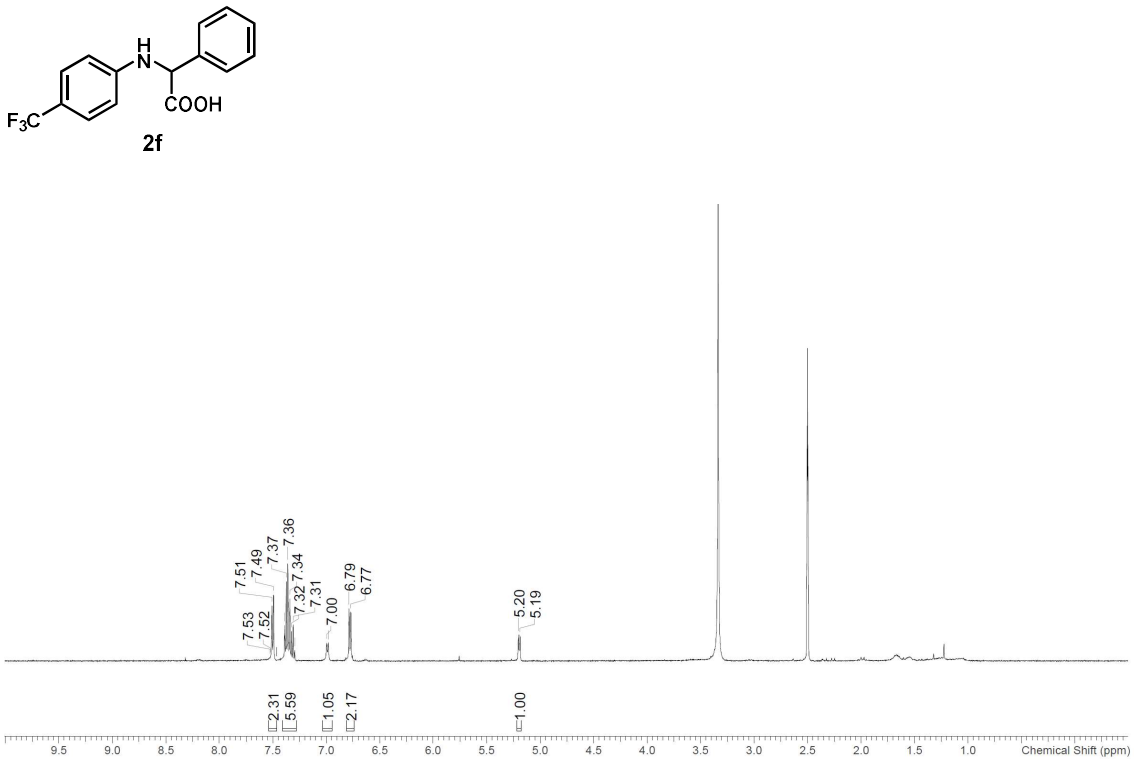

Fig. S31 ^{1}H NMR (500 MHz, DMSO-d_6) spectrum of α-[(4-trifluoromethylphenyl)amino]-benzeneacetic acid (**2f**).

15. Supporting references

1 Y. Arroyo, M. A. Sanz-Tejedor, I. Alonso and J. L. García-Ruano, *Org. Lett.*, 2011, **13**, 4534–4537.

2 G. P. Junor, E. A. Romero, X. Chen, R. Jazzar and G. Bertrand, *Angew. Chemie - Int. Ed.*, 2019, **58**, 2875–2878.

3 M. Durán-Galván and B. T. Connell, *Tetrahedron*, 2011, **67**, 7901–7908.

4 C. Faggi, A. G. Neo, S. Marcaccini, G. Menchi and J. Revuelta, *Tetrahedron Lett.*, 2008, **49**, 2099–2102.

5 Y. Naito, Y. Nakamura, N. Shida, H. Senboku, K. Tanaka and M. Atobe, *J. Org. Chem.*, 2021, **86**, 15953–15960.

6 A. V. Kurkin, N. E. Golantsov, A. V. Karchava and M. A. Yurovskaya, *KHIMIYA GETEROTSIKLICHESKIKH SOEDINENII*, 2003, **39**, 78–86.

7 Z. Lu and R. J. Twieg, *Tetrahedron Lett.*, 2005, **46**, 2997–3001.

8 A. A. Sathe, D. R. Hartline and A. T. Radosevich, *Chem. Commun.*, 2013, **49**, 5040–5042.

9 R. G. Compton, A. C. Fisher, R. G. Wellington, P. J. Dobson, and P. A. Leigh, *J. Phys. Chem.,* 1993, **97**, 10410–10415.

10 C. A. Paddon, G. J. Pritchard, T. Thiemann, and F. Marken, *Electrochem. Commun.,* 2002, **4**, 825–831.